Poly(Cyano-Substituted Diheteroareneethylene) as Active Electrode Material for Electrochemical Supercapacitors

Florence Fusalba,[†] Hoang Anh Ho,[‡] Livain Breau,*[,‡] and Daniel Bélanger*[,†]

Département de Chimie and Laboratoire de Synthèse Organique Appliquée, Département de Chimie, Université du Québec à Montréal, Case Postale 8888, succursale Centre-Ville, Montréal (Québec) Canada, H3C 3P8

Received January 5, 2000. Revised Manuscript Received July 7, 2000

A new class of low band gap thiophene polymers prepared from (*E*)-α-cyanoethylene thiophene derivatives were electrochemically and physically evaluated as active electrode material for electrochemical supercapacitors. The corresponding polymers were prepared by electrochemical polymerization of these monomers from a nonaqueous solution (acetonitrile) containing tetraethylammonium tetrafluoroborate. The electrochemical properties and the stability under cyclic voltammetry of the polymers were found to be strongly dependent on their electronic configuration, especially in the case where the monomer has two different aromatic heterocycles. The range of stable electroactivity of the polymers in organic media spans about 2 V. Since poor stability was observed by cyclic voltammetry for poly-(*E*)-α-[(2-thienyl)methylene]-2-(3-methylthiophene)acetonitrile and poly-(*E*)-α-(2-thienylmethylene)-2-furanacetonitrile, only poly-(*E*)-α-[(2-thienyl)methylene]-2-thiopheneacetonitrile, poly-(*E*)-α-[(3-methyl-2-thienyl)methylene]-2-thiopheneacetonitrile, and poly-(*E*)-α-[(2-furanyl)methylene]-2-thiopheneacetonitrile were evaluated as electrode materials for an electrochemical supercapacitor. Stability tests upon potential cycling between the n- and p-doped states and a potential range of about 2 V have shown a 60% decrease of the voltammetric charge for poly-(*E*)-α-[(2-thienyl)methylene]-2-thiopheneacetonitrile following 2000 cycles. Preliminary galvanostatic charge−discharge cycling experiments for the best system indicated an energy density of 8.6 W h/kg while it delivered a power density of 1.6 kW/kg for a discharge time of 20 s.

Introduction

Conducting polymers derived from monomers such as pyrrole, aniline, and thiophene have attracted a lot of interest in the past two decades because these materials possess potential applications as active electrode material in lightweight rechargeable batteries and electrochemical supercapacitors.[1−4] The realization of high energy and power density polymer supercapacitors requires conducting polymers which can be n- and p-doped over a potential window of 2−3 V.[5−8] It has been shown that polythiophene-based electrochemical supercapacitors can generate such a cell voltage, but their n-doping process suffers from some serious drawbacks: the polymers are generated from monomers under high oxidative potential which can irreversibly oxidize the polymer being generated,[9] a low ratio between the n- and p-doping level has been reported,[10] a region of low conductivity is observed between the n- and p-doped states for the polymer,[11] and some irreversible phenomena take place when the n-doping process is performed.[12] Presumably, these aforementioned drawbacks can be minimized by using, as active electrode materials, low band gap polythiophene derivatives displaying n-doping processes at less negative potentials.[13−16]

* To whom correspondence should be sent. E-mail: belanger.daniel@uqam.ca and breau.livain@uqam.ca.

[†] Département de Chimie.

[‡] Laboratoire de Synthèse Organique Appliquée, Département de Chimie.

(1) *Handbook of Conducting Polymers*; Skotheim, T., Elsenbaumer, R. L., Reynolds, J. R., Eds.; Marcel Dekker: New York, 1998.

(2) *Handbook of Organic Conductive Molecules and Polymers: Transport, Photophysics and Applications*; Nalwa, H. S., Ed.; Wiley: New York, 1997; Vol. 4.

(3) Novak, P.; Muller, K.; Santhanam, K. S. V.; Hass, O. *Chem. Rev.* **1997**, *97*, 207.

(4) (a) Miller, J. S. *Adv. Mater.* **1993**, *5*, 587. (b) Miller, J. S. *Adv. Mater.* **1993**, *5*, 671.

(5) Arbizzani, C.; Mastragostino, M.; Scrosati, B. *Handbook of organic conductive molecules and polymers*; Nalwa, H. S., Ed.; Wiley: New York, 1997, Vol. 4, p 595.

(6) Arbizzani, C.; Mastragostino, M.; Meneghello, L.; Paraventi, R. *Adv. Mater.* **1996**, *8*, 331.

(7) Rudge, A.; Davey, J.; Raistrick, I.; Gottesfeld, S.; Ferraris, J. P. J. *Power Sources* **1994**, *47*, 89.

(8) Rudge, A.; Raistrick, I.; Gottesfeld, S.; Ferraris, J. P. *Electrochim. Acta* **1994**, *39*, 273.

(9) Chayer, M.; Faïd, K.; Leclerc, M. *Chem. Mater.* **1997**, *9*, 2902.

(10) Beyer, R.; Kalaji, M.; Kingscote-Burton, G.; Murphy, P. J.; Pereira, V. M. S. C.; Taylor, D. M.; Williams, G. O. *Synth. Met.* **1998**, *92*, 25.

(11) Ferraris, J. P.; Eissa, M. M.; Brotherston, I. D.; Loveday, D. C.; Moxey, A. A. *Electroanal. Chem.* **1998**, *459*, 57.

(12) Zotti, G.; Schiavon, G.; Zecchin, S. *Synth. Met.* **1995**, *72*, 275.

(13) Fusalba, F.; El Mehdi, N.; Breau, L.; Bélanger, D. *Chem. Mater.* **1999**, *11*, 2743.

(14) *Handbook of Conducting Polymers*; Skotheim, T., Elsenbaumer, R. L., Reynolds, J. R., Eds.; Marcel Dekker: New York, 1998; p 277.

(15) (a) Roncali. J. *Chem. Rev.* **1992**, *92*, 711. (b) Roncali, J. *Chem. Rev.* **1997**, *97*, 173.

(16) Roncali, J. *J. Mater. Chem.* **1999**, *9*, 1875.

10.1021/cm000011r CCC: $19.00
Published on Web 08/31/2000

Chart 1. Structure of the Oligomers

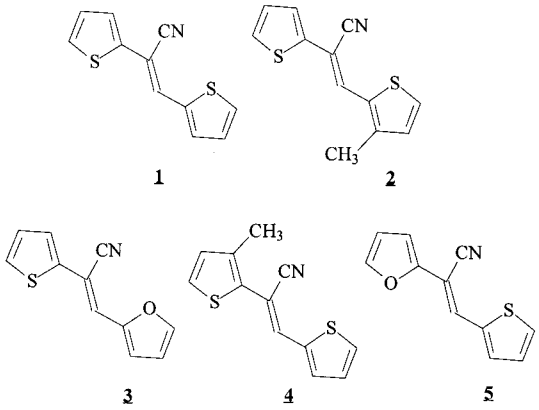

Scheme 1. Monomer Synthesis

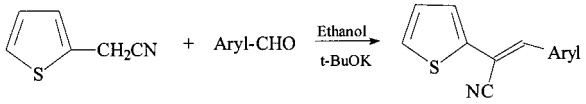

Scheme 2. Synthesis of 2-Arylacetonitriles

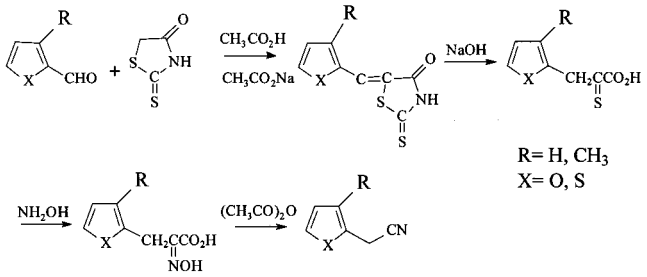

Roncali et al.[17,18] have recently shown that the introduction of a cyano group to the ethylene linkage of poly(diarylenevinylene) produces a significant increase in its electron affinity. In their initial study, they showed that poly(thienylenevinylene) has a lower band gap (E_{gap}) than polythiophene, since ethylene linkages of defined conformation reduce the aromatic character of the π-conjugated backbone.[17] They also reported that the association of furan with thiophene prevents the anodic overoxidation of the furan. In another study, Roncali et al.[18] have synthesized a series of π-conjugated oligomers containing three-, four-, and five-membered heterocycles and two CN groups at various positions with respect to the ethylene linkage. They showed that the introduction of CN groups leads to a considerable positive shift in reduction potential and that the number and reversibility of the reduction steps strongly depend on the position of the CN groups and on the length of the oligomer.

Zotti et al.[19] have investigated polyconjugated polymers containing pyrrole and thiophene units bridged by a cyanoethylene group and have found that the introduction of a cyano group leads to a decrease in the band gap as well as the conductivity of the polymer. On the other hand, the position of the cyano group on a dipyrrolyl−ethylene polymer strongly influences its optical properties whereas its electronic conductivity was barely affected due to the fact that the intersite hopping distance is not affected. Reynolds et al.[20] also incorporated a cyano group into the vinylene unit of electron rich poly(bis(heterocycle)vinylene) systems to afford low band gap polymers. They found that the band gaps of poly(1-cyano-2-(2-(3,4-ethylenedioxythienyl))-1-(2-thienyl)vinylene) and poly(1-cyano-1,2-bis(2-(3,4-ethylenedioxythienyl))vinylene) are 1.3 and 1.1 eV, respectively, and their polymers can be p-doped and reversibly reduced over a potential range of about 3 V.

Although the grafting of a cyano group onto the ethylene linkage was investigated by the aforementioned groups, the effect of such a graft is not yet fully understood. As a natural extension of this research, we report here the synthesis of a set of new oligomers (**4** and **5**) and a comparison with the oligomers (**1**, **2**, and **3**) originally developed by Roncali[17] (see Chart 1). These new oligomers were chosen so as to limit permutation to the CN group and the olefinic proton of the structure (e.g. **2** compared with **4**, and **3** compared with **5**). In this paper, we also report the electrochemical synthesis of several polythienylethylene derivatives (poly-**1** to poly-**5**) along with their characterization by electrochemical (cyclic voltammetry and electrochemical impedance spectroscopy) and spectroscopic (UV/visible) techniques. The morphology of the resulting polymers was also characterized by scanning electron microscopy. Finally, polymers displaying good electrochemical stability, especially in their n-doped state, were tested by constant current charge−discharge cycling in order to evaluate their potential as active electrode materials in electrochemical supercapacitors.

Results and Discussion

Synthesis of the Monomers. The synthesis of monomers **1**−**3** involves a Knoevenagel condensation between 2-thiopheneacetonitrile and the appropriate 2-arylaldehyde in the presence of potassium *tert*-butoxide (Scheme 1). A series of monomers was thus prepared by varying the aryl groups including thiophene and furane with or without a substituent in the β-position (Scheme 1). The synthesis of 2-furanacetonitrile and 2-(3-methylthiophene)acetonitrile, required for the synthesis of monomers **4** and **5**, was carried out in several steps according to Julian's method[21,22] (Scheme 2). The first step was the condensation of a 2-arylaldehyde with rhodanine, which gave the corresponding 2-arylmethylidenerhodanine. After saponification, these compounds yielded 3-aryl-2-thioketopropionic acids. These acids were treated with hydroxylamine to provide the corresponding oximes, which were dehydrated further with acetic anhydride to provide the corresponding 2-arylacetonitriles.

Characterization of the Monomers. Table 1 shows the main optical and electrochemical data of **1**−**5**. The anodic peak potential values for **1**−**3** are in good agreement with those reported earlier by Roncali et al.[17] and are consistent with the variation of the absorption

(17) Ho, H. A.; Brisset, H.; Frère, P.; Roncali, J. *J. Chem. Soc., Chem. Commun.* **1995**, 2309.
(18) Ho, H. A.; Brisset, H.; Elandaloussi, E. H.; Frère, P.; Roncali, J. *Adv. Mater.* **1996**, *8*, 990.
(19) Zotti, G.; Zecchin, S.; Schiavon, G.; Berlin, A.; Pagani, G.; Borgonovo, M.; Lazzaroni, R. *Chem. Mater.* **1997**, *9*, 2876.
(20) Sotzing, G. A.; Thomas, C. A.; Reynolds, J. R.; Steel, P. J. *Macromolecules* **1998**, *31*, 3750.
(21) Julian, P. L.; Sturgis, B. M. *J. Am. Chem. Soc.* **1935**, *57*, 1126.
(22) Plucker, J.; Amstuts, E. D. *J. Am. Chem. Soc.* **1940**, *62*, 1512.

Table 1. Electrochemical and UV−Visible Absorption Data for the Monomers

monomer	λ_{max}[a]/UV (nm)	E_{pa} (V vs Ag/Ag$^+$)[b]
1	368	1.1
2	374	1.03
3	364	0.97
4	358	1.08
5	369	1.05

[a] Maximum absorption, λ_{max}, for a 10^{-6} M concentration in $CHCl_3$. [b] Anodic peak potential, E_{pa}, at a platinum electrode for a 10^{-6} M monomer, 0.1 M Et_4NBF_4/acetonitrile solution at a scan rate of 100 mV/s.

maximum of their corresponding monomer solutions. The blue-shifted absorption maximum for monomer **4** relative to **2** demonstrates the influence of monomer substitution pattern on absorption and might be related to a deviation from planarity induced by the steric hindrance of the methyl and cyano groups in **4**. This is also consistent with the observation of a higher oxidation peak potential for **4** as compare to **2**. Preliminary PM3 calculations have indicated that monomer **4** is slightly more distorted than **2**. On the other hand, Table 1 shows that the anodic peak potential for **5** is at a more positive value than that for **3**. This is in agreement with PM3 calculations suggesting that **3** is more planar than **5** and hence that the reactivity of the monomers is different. On the other hand, the red-shifted absorption maximum for monomer **5** as compared to **3** is unclear for the moment, but it should be kept in mind that some caution is needed due to the relatively small difference in λ_{max} values. The data presented above seem to suggest that there is a small effect of the position of the CN group of the ethylene linkage and of the nature of the heterocycle linked to the ethylene linkage, but a more dramatic effect was observed for the polymers grown from these monomers (vide infra).

Characterization of the Polymers by Cyclic Voltammetry. A typical cyclic voltammogram between −1.3 and 0.6 V of an as-grown poly-**1** in 1 M Et_4NBF_4/acetonitrile is shown as an inset of Figure 1 (solid line). It is characterized by two sets of well-defined redox waves centered at 0.3 and − 0.7 V associated with the p- and n-doping redox reactions, respectively. The shape of these cyclic voltammograms (CV's) is similar to that reported by Roncali et al.[17] CV 1 also shows cathodic and anodic prepeaks around −0.4 and 0.2 V, respectively, for the n-doping and p-doping processes. These prepeaks can be attributed to charge-trapping phenomena[12] and have been further investigated using electrochemical impedance spectroscopy, EIS (vide infra). The data shown in Figure 1 demonstrate that poly-**1** can be cycled between n- and p-doping states over a potential window of about 2 V. From these data, the cell voltage developed by a poly-**1**-based electrochemical supercapacitor would be close to 2 V.[5,7] In addition, the inset of Figure 1 indicates that 40% of the initial voltammetric charge of poly-**1** remained after 2000 cycles, performed at a scan rate of 100 mV/s. Figure 1 also displays the CV of poly-**1** for an extended potential range. The irreversible wave observed at around −1.5 V was not reported by Roncali et al.[17] On the other hand, a similar reduction wave was attributed to the reduction of the polymer for a cyanovinylene polymer based on ethylenedioxythiophene.[20] However, a partially reversible wave has been reported by Zotti et al. in this potential

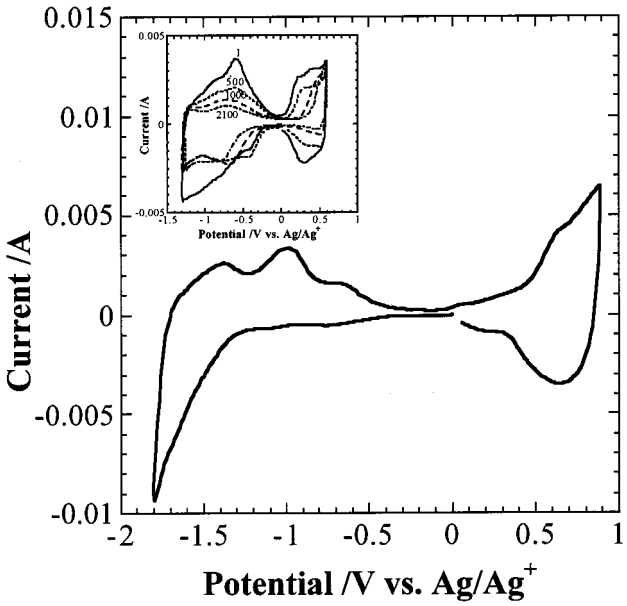

Figure 1. Cyclic voltammogram of poly-**1** ($Q_{deposited}$ = 0.2 C/cm^2) on a carbon paper electrode in 1 M Et_4NBF_4/acetonitrile for an extended potential range. Scan rate 100 mV/s. Growth conditions: 20 mM [**1**], 1 M Et_4NBF_4/acetonitrile, 0.1 mA/cm^2. Inset: Cyclic voltammogram of poly-**1** ($Q_{deposited}$ = 0.2 C/cm^2) on a carbon paper electrode in 1 M Et_4NBF_4/acetonitrile at a scan rate of 100 mV/s. Growth conditions: 20 mM [**1**], 1 M Et_4NBF_4/acetonitrile, 0.1 mA/cm^2. Cycles: 1 to 2100.

region for poly(2,5-bis[1-cyano-2-(pyrrol-2-yl)vinyl]thiophene) which was attributed to the electron-withdrawing effect of the cyano group.[19] The same authors have also proposed that the partially reversible reduction process is followed by hydrodimerization of the polymers.[19] It will be shown below, in the section dealing with EIS, that the resulting polymer displays some electroactivity and maintains some charge storage ability despite this irreversible chemical process. The electrochemical band gap estimated from the data shown in Figure 1, and calculated from the difference between the threshold potentials for p- and n-doping, is about 0.5 eV and is in agreement with that previously reported by Roncali et al.[17]

The electrochemical behavior of poly-**2**, which bears a methyl group on a thiophene unit, ressembles that of poly-**1** (see Figures 1 and 2 of the Supporting Information and Table 2). The electrochemical band gap is about 1.5 eV and is in agreement with that reported by Roncali,[17] but a lower band gap value of 0.4 eV can be evaluated for poly-**2** if the CV is analyzed similarly to that of the inset of Figure 1. Monomer **4**, having a cyano group close to the methyl-substituted thiophene unit, can also be electropolymerized on a carbon paper electrode, and the CV of the resulting polymer (Figure 3 of the Supporting Information) is characterized by redox waves at about the same potentials as those of poly-**2** (Table 2). The optical band gap energy is slightly lower for poly-**4** than poly-**2**, and the absorption maximum of poly-**4** (523 nm) is red-shifted compared to that of poly-**2** (505 nm), which is in contrast to the band gap energies predicted by the optical spectra of the corresponding monomers. The discrepancy might be due to steric interactions in the polymer. On the other hand, the increase in the conjugation length of poly-**4** relative to poly-**2** might be attributed to the higher reactivity of

Table 2. Electrochemical and UV−Visible Absorption Data for the Polymer.

polymer[a] (poly-), [monomer] (mM)	λ_{max}/UV[b] (nm)	E_{stab}[a] (V vs Ag/Ag$^+$)	E_g/UV[c] (eV)	E /CV[d] (eV)	E_{pa}[e] (V vs Ag/Ag$^+$)	E_{pc}[f] (V vs Ag/Ag$^+$)	Q_{p^+}/Q_{p^-}[g] (mC/cm^2)	Q_{n^+}/Q_{n^-}[g] (mC/cm^2)	x_p/x_n[h]
1, 20	531	0.82	0.54	0.5	0.7	−1.6	22/16	25/19	0.12/0.11
2, 10	505	0.77	1.55	1.5, 0.4	0.7	−1.6	23/21	17/16	0.13/0.09
3, 20	511	0.71	1.4	1.4	0.5	−1.5	14/12	9/10	0.08/0.05
4, 90	523	0.74	<1.5	1.4	0.7	−1.6	8/5	9/12	0.04/0.06
5, 20	508	0.73	<1.4	1.38	0.7	−1.5	9/6	9/13	0.05/0.07

[a] Deposition conditions: i = 0.1 mA/cm^2, deposited charge = 200 mC/cm^2 on 1 cm^2 carbon paper electrodes. Supporting electrolyte: 1 M Et_4NBF_4/acetonitrile. E_{stab} = stabilization potential during galvanostatic deposition. [b] Absorption maximum wavelengths of the optical spectra of undoped polymers. Deposition conditions: i = 0.5 mA/cm^2, deposited charge = 20 mC/cm^2 on ITO electrodes. Supporting electrolyte: 0.1 M Et_4NBF_4/acetonitrile. Potential used for the polymer neutralization: 0 V versus Ag/Ag$^+$ for 50 s. [c] Band gap, E_g/UV, estimated from the absorption onset of the optical spectra of undoped polymers. Deposition conditions: i = 0.5 mA/cm^2, deposited charge = 20 mC/cm^2 on ITO electrodes. Supporting electrolyte: 0.1 M Et_4NBF_4/acetonitrile. Potential used for the polymer neutralization: 0 V versus Ag/Ag$^+$ for 50 s. [d] Band gap, E_g/UV, estimated from the potential difference between the onsets for the oxidation and reduction waves of the cyclic voltammogram. Electrolyte: 1 M Et_4NBF_4/acetonitrile. [e] p-doping anodic peak potential, E_{pa}. [f] n-doping cathodic peak potential, E_{pc}. [g] Q_{p^+} = p-doping oxidation charge. Q_{p^-} = p-doping reduction charge. Q_{n^+} = n-doping oxidation charge. Q_{n^-} = n-doping reduction charge. [h] Doping level, x, calculated from $x = (Q_{CV}/Q_{dep})/(1 - (Q_{CV}/Q_{dep}))$, with $Q_{CV} = Q_{p^+}$ or Q_{n^-} and assuming a polymerization efficiency of 100%.

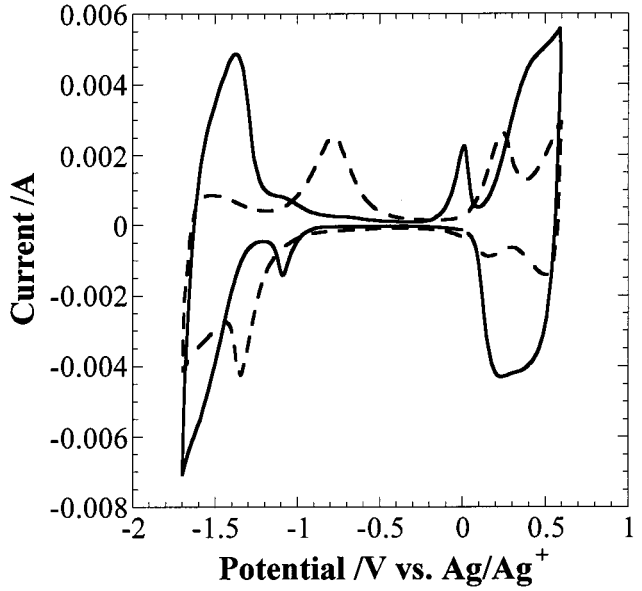

Figure 2. Cyclic voltammogram of poly-**3** (—) and poly-**5** (- - -) ($Q_{deposited}$ = 0.2 C/cm^2) on a carbon paper electrode in 1 M Et_4NBF_4/acetonitrile at a scan rate of 100 mV/s. Growth conditions: 20 mM [**3** or **5**], 1 M Et_4NBF_4/acetonitrile, 0.1 mA/cm^2.

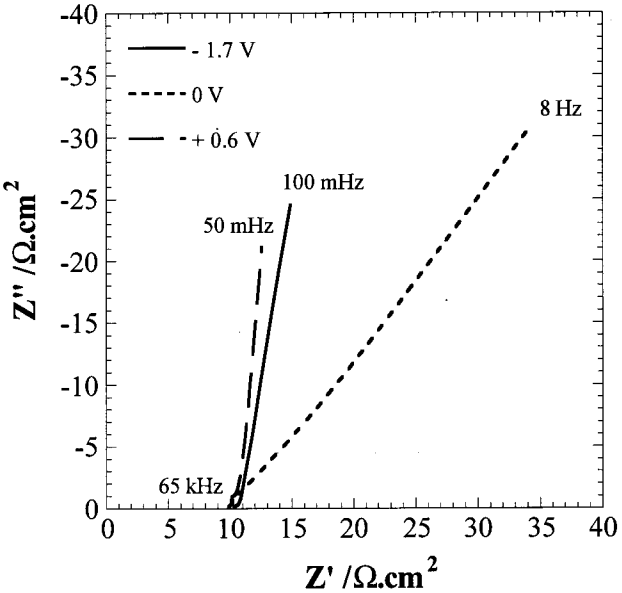

Figure 3. Complex plane impedance plots for a poly-**3** film coated carbon paper electrode at −1.7 V (—), 0 V (···), and 0.6 V (— · —) in 1 M Et_4NBF_4/acetonitrile solution. Deposition conditions: 20 mM [**3**], 1 M Et_4NBF_4/acetonitrile, 0.1 mA/cm^2, $Q_{deposited}$ = 1 C/cm^2.

the radical cations of monomer **4**. The latter is evidenced by a more positive anodic peak potential for **4** (Table 1). Thus, the position of the cyano group affects the electrochemical behavior of the resulting polymers.[18] Indeed, Roncali et al.[18] have shown that the reversibility and the anodic and cathodic peak potentials of the oligomers and the polymers were influenced by the position (inner versus outer) of the CN substituent of the ethylene linkage. Unfortunately, poly-**4** was less stable than poly-**2** upon potential cycling. This might be attributed to the influence of the cyano group in poly-**4** relative to poly-**2**.

The substitution of a thiophene unit by furan in **1** strongly influenced the cyclic voltammetry of the polymer. The CV of poly-**3** (Figure 2, curve —) is characterized by two sets of redox waves centered at −1.5 and 0.4 V for the n- and p-doping processes, respectively, in addition to well-defined prepeaks attributed to trapped charges. The band gap value of 1.4 eV estimated from the CV is in good agreement with that obtained from the optical spectrum as well as that reported by Roncali et al.[17] The CV of poly-**3** differs from those discussed above in that it does not exhibit less intense redox waves between the main p- and n-doping processes. The lack of redox activity might be primarily due to the better reversibility of the n-doping redox reaction of poly-**3** and to its larger band gap. The better reversibility for the n-doping process of poly-**3** is evidenced by the observation of the n-dedoping wave at less positive potential.

In contrast, poly-**5** exhibited two redox waves for the n- and p-doped states centered at −1.5 and 0.7 V (Figure 2, curve - - - and Table 2), respectively, which were less intense than the redox waves found for poly-**1**, -**2**, and -**3**. Interestingly, the n-doping process was less reversible when the cyano group was close to the furanyl unit (see CV's for poly-**5** and poly-**3**), whereas the p-doping process maintained its reversibility. In addition, the p-doping redox waves for poly-**5** were shifted toward more anodic potentials in comparison to those observed for poly-**3**. This suggests an enhanced inductive electronic effect for the oxygen atom which in turn increases the HOMO level. However, poly-**3** and -**5** have similar

band gaps due to an increase in the LUMO level for poly-**5**. Finally, poly-**5** lacks the long-term stability of poly-**3** under potential cycling and is thus less interesting for electrochemical supercapacitor applications. The decreased stability of poly-**5** might be linked to the irreversibility of the n-doping process. On the other hand, polyfuran is known to be chemically unstable, particulary in the oxidized state.[24,25] It readily undergoes ring opening in the presence of nucleophiles such as traces of water or BF_4^- anions. It seems that the irreversible reaction is favored when the cyano group is closer to the furan ring (poly-**5**). In addition, UV−visible spectroscopy indicates a blue-shift of the absorption maximum (λ_{max}) for poly-**5** compared to poly-**3**. This is in contrast to the λ_{max} of the corresponding monomers. Therefore, it can be concluded that poly-**5** has a shorter conjugation length than poly-**3**. This effect may be attributed to the instability of the furan ring, which is a more electron dense functionality. However, this might be linked to the fact that monomer **3** is more planar than monomer **5** according to PM3 calculations. Moreover, the dihedral angle between the double bond and the thiophene ring is indeed larger in **5**.

The voltammetric charges for p-doping (p^+), p-dedoping (p^-), n-doping (n^-), and n-dedoping (n^+) were obtained by integration of the CV's of the various polymers and are included in Table 2. The charges of poly-**1**, -**2**, and -**3** are slightly higher than those of poly-**4** and -**5**, suggesting that the polymerization efficiency is lower for poly-**4** and -**5**. In addition, the doping/dedoping ratios are more balanced for poly-**1**, -**2**, and -**3**, and these polymers also showed higher stability. An unbalanced doping/dedoping ratio is an indication that irreversible processes are occurring during the redox process, as was observed for poly-**4** and -**5**. The doping level, *x*, estimated for both p- and n-doped states (see Table 2) by assuming a polymerization efficiency of 100%, is fairly low (0.05−0.13) in comparison to those usually found for polythiophenes.[8,26,27] Presumably, these doping levels are underestimated, since the polymerization efficiency is probably lower than 100% and since the electrolyte became colored during the electropolymerization. Indeed polymerization efficiencies of about 70% have recently been reported for other polythiophene derivatives.[26]

Electrochemical Impedance Spectroscopy, EIS, of Polymers. EIS was used to evaluate the low-frequency capacitance of the polymer electrodes. Figure 3 shows the complex impedance plots (Z'' vs Z') for a poly-**3**-coated carbon paper electrode in oxidized, neutral, and reduced states. For both the oxidized ($E = 0.6$ V) and the reduced ($E = -1.7$ V) forms, the low-frequency data lie on an almost vertical line, as expected for a system displaying a capacitive behavior.

The capacitance is calculated from the slope of a plot of the imaginary component of the impedance, at low frequency, as a function of the reciprocal of the frequency.[29] Figure 4 depicts the capacitance−potential plots for poly-**1** and -**3**, and it can be seen that their shapes correlate well with those of the corresponding anodic branch of the cyclic voltammograms except that no prepeaks are observed on the low-frequency capacitance plots. This can clearly be seen when one compares the cyclic voltammogram (Figure 2, curve —) and the capacitance−potential plot (Figure 4, curve - - -) for poly-**3**. The lack of prepeaks was previously observed for the polycyclopenta[2,1-*b*;3,4-*b*′]dithiophen-4-one[13] and was considered evidence that most of the charge associated with the prepeaks of the CV is trapped charge.[30−35] This trapped charge cannot be detected by EIS because the polymer electrode is polarized for a sufficient time prior to the measurements to allow the release of the trapped charge.[13]

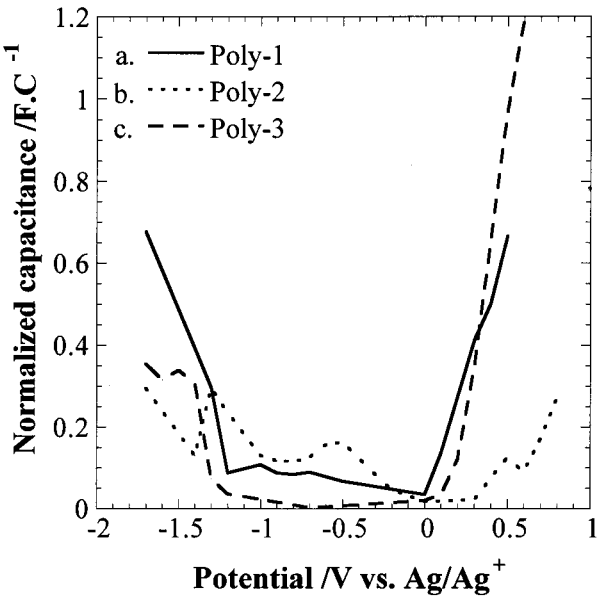

Figure 4. Low-frequency capacitance of poly-**1** (—); poly-**2** (···), and poly-**3** (- - -) on carbon paper electrodes as a function of potential in 1 M Et_4NBF_4/acetonitrile. Deposition conditions: 20 mM [**1**], 1 M Et_4NBF_4/acetonitrile, 0.1 mA/cm^2, $Q_{deposited} = 1$ C/cm^2); 10 mM [**2**], 1 M Et_4NBF_4/acetonitrile, 0.1 mA/cm^2, $Q_{deposited} = 0.2$ C/cm^2); and 20 mM [**3**], 1 M Et_4NBF_4/acetonitrile, 0.1 mA/cm^2, $Q_{deposited} = 1$ C/cm^2).

The capacitances for poly-**2** are quite similar to those of poly-**1** at the positive and negative potential limits when corrected for the same deposition charge. The slightly higher capacitance between −0.4 and −1 V for poly-**2** is consistent with the relatively intense voltammetric waves observed on the CV of poly-**2**. On the other hand, poly-**3** displays higher capacitance in the p-doped state (160 mF/cm^2 or 160 F/g) than in the n-doped state

(23) Silverstein, R. M.; Bassler, G. C.; Morrill, T. C. *Spectrometric Identification of Organic Compounds*; John Wiley & Sons Inc.: New York, 1991; p 312.
(24) Benahmed-Gasmi, A.; Frère, P.; Roncali, J. *J. Electroanal. Chem.* **1996**, *406*, 231.
(25) Glenis, S.; Benz, M.; Legoff, E.; Schindler, J. L.; Kannewurf, C. R.; Kanatzidis, M. G. *J. Am. Chem. Soc.* **1993**, *115*, 12519.
(26) Ferraris, J. P.; Eissa, M. M.; Brotherston, I. D.; Loveday, D. C. *Chem. Mater.* **1998**, *10*, 3528.
(27) Gofer, Y.; Killian, J. G.; Sarker, H.; Poehler, T. O.; Searson, P. C. *J. Electroanal. Chem.* **1998**, *443*, 103.
(28) Crooks, R. M.; Chyan, O. M.; Wrighton, M. S. *Chem. Mater.* **1989**, *1*, 2.
(29) Fiordiponti, P.; Pistoia, G. *Electrochim. Acta* **1989**, *34*, 215.
(30) Abruna, H. D.; Denisevich, P.; Umana, M.; Meyer, T. J.; Murray, R. W. *J. Am. Chem. Soc.* **1981**, *103*, 1.
(31) Denisevich, P.; Abruna, H. D.; Leider, C. R.; Meyer, T. J.; Murray, R. W. *Inorg. Chem.* **1982**, *21*, 2153.
(32) Berthelot, J. R.; Angely, L.; Delaunay, J.; Simonet, J. *New J. Chem.* **1987**, *11*, 487.
(33) Borjas, R.; Buttry, D. A. *Chem. Mater.* **1991**, *3*, 872.
(34) Zhou, Z.; Maruyama, T.; Kanbara, T.; Ikeda, T.; Ichimura, K.; Yamamoto, T.; Tokuda, K. *J. Chem. Soc., Chem. Commun.* **1991**, 210.
(35) Gottesfeld, S.; Redondo, A.; Rubinstein, I.; Feldberg, S. W. *J. Electroanal. Chem.* **1989**, *265*, 15.

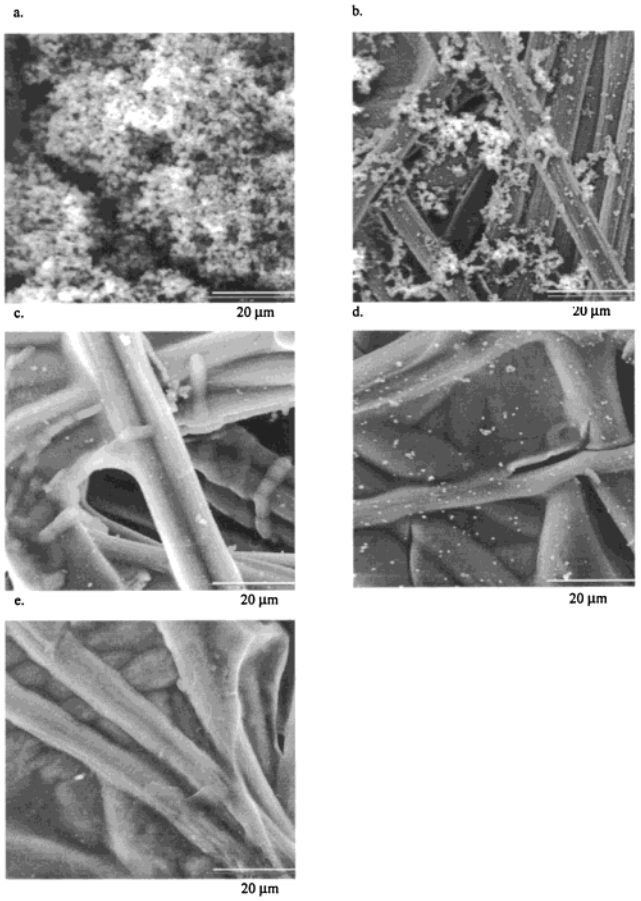

Figure 5. Scanning electron micrographs of (a) a poly-**1**-coated carbon paper electrode (×1500, 20 kV), (b) a poly-**2**-coated carbon paper electrode (×1500, 5 kV); (c) a poly-**3**-coated carbon paper electrode (×1500, 20 kV), (d) a poly-**4**-coated carbon paper electrode (×1500, 5 kV), and (e) a poly-**5** film grown on carbon paper (×1500, 5 kV). Deposited charge: 1 C/cm^2.

(40 mF/cm^2 or 40 F/g). In its n-doped state, the low-frequency capacitance of poly-**5** compares well with that of poly-**3** (the latter is slightly lower). However, its chemical instability in the oxidized state does not allow any EIS measurements, since the polymer is degraded during the experiments. Conversely, poly-**4** displays lower capacitances than poly-**2** for the p-doping process while the n-doping low-frequency capacitance cannot be collected due to loss of stability in the reduced state of poly-**4**. Therefore, the change in the electronic configuration for monomers **4** and **5** reduced the polymerization efficiency of the corresponding polymers. The presence of soluble oligomers within the π-conjugated polymer system was supported by UV−visible spectroscopy. These species can subsequently be leached out of the polymer layer, which leads to smaller low-frequency capacitance values. Moreover, the film stability in fully reduced or oxidized states is dramatically lowered.

Scanning Electron Microscopy. Photomicrographs were obtained for poly-**1**−**5** films grown on carbon paper (Figure 5). The morphologies of poly-**1** and -**2** films (Figure 5a and b) consist of small globular particles with an open and rough structure whereas those of poly-**3**, -**4**, and -**5** (Figure 5c−e) are more compact and uniform. The photomicrograph for poly-**3** (×1500) is characterized by carbon fibers coated with polymer aggregates growing both perpendiculary and around the fibers. The film

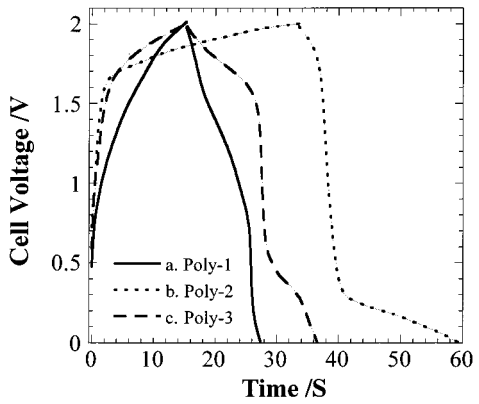

Figure 6. Variation of the potential with time during constant current (0.5 mA/cm^2 for poly-**1** and poly-**3** but 0.3 mA/cm^2 for poly-**2**) cycling of a poly-**1** (—), poly-**2** (···), or poly-**3** (- - -) capacitor (2 electrodes). The capacitor assembled with poly-**2** or poly-**3** was maintained at 2 V for 100 s after the charging step (not shown) while the poly-**3**-based capacitor was cycled between −2 and 2 V. Electrolyte: 1 M Et_4NBF_4/acetonitrile. The deposited charge is 0.2 C/cm^2 for poly-**1** and poly-**3** but 2 C/cm^2 for poly-**2**.

morphology of poly-**4** is more compact than that of poly-**2**, and poly-**4** also appears to grow on top of the carbon paper electrode.

Galvanostatic Charge−Discharge Cycling. Constant current charge−discharge cycling between 0 V and a maximum cell voltage of 2 V was performed on capacitors assembled from poly-**1**-, -**2**-, and -**3**-coated carbon paper electrodes in 1 M Et_4NBF_4/acetonitrile (Figure 6). Poly-**4** and -**5** were not tested by galvanostatic cycling, since these polymers were shown to have limited cyclic voltammetry stability. The stability of a poly-**1**, -**2**, or -**3**-based electrochemical supercapacitor upon cycling was evaluated, and the discharge capacity decreased to 50, 35, and 8% of the initial value, respectively, between the first and the 100th cycle. A maximum discharge capacity of 7 mAh/g of electroactive polymer (Table 3) was calculated from the discharge curve for poly-**3**, which is less than 6% of the theoretical value. In addition, the discharge capacity was found to be similar to those found for devices based on poly[3-(phenylthiophene)] derivatives (10 mAh/g),[26] poly(3,5-difluorophenylthiophene)/poly(3,4,5-trifluorophenylthiophene) (10 mAh/g),[27] and poly(cyclopenta[2,1-*b*;3,4-*b*′]dithiophen-4-one) (6 mAh/g).[13]

The charge cycling efficiency, defined as the ratio of the energy delivered by the capacitor upon discharge to that needed to charge it, is close to 100% (Table 3). The charge cycling efficiency of 120% obtained for poly-**3**-based capacitors is due to the fact that the capacitor was held at 2 V for 100 s after the charging step and that the corresponding charge is not taken into account in the calculation. Since the potential was set at 2 V for 100 s before the discharge, a higher amount of active material was thereafter addressed. The energy densities, E, for poly-**1** and -**3** capacitors were respectively 4.4 and 8.6 W h/kg of active material. The power densities, P, were respectively 1.3 and 1.6 kW/kg for poly-**1** and -**3** capacitors, for a discharge time of about 10−20 s. Thus, comparable E and P values were reported for capacitors using a fairly low polymer loading of 0.2 C/cm^2 on each electrode. Unfortunately, the energy and power densities decreased significantly

Table 3. Charge−Discharge Data for Poly-1-, -2-, and -3-Based Capacitors

poly-	Q_{dep} (C/cm^2)	m_{th}[a] (g)	I[b] (mA/cm^2)	Q_{th}[c] (mA h/g)	Q_{exp}[d] (mA h/g)	charge cycling efficiency (%)	E[e] (W h/kg)	P[f] (W/kg)	t[g] (s)
1	0.2	0.000 45	0.5	247	4.5	83	4.4	1300	12
2	2	0.004 78	0.3	232	0.9	77	0.25	35	25
3	0.2	0.000 42	0.5	266	7	120	8.6	1600	19

[a] Calculated mass of undoped polymer for 2 cm^2 electrodes assuming a polymerization yield of 100%. [b] Current density used to charge−discharge the capacitor. [c] Theoretical capacity. [d] Experimental capacity. [e] Energy density. [f] Power density. [g] Discharge time.

to 0.25 W h/kg and 35 W/kg when thicker poly-**2** films were used (deposited charge = 2 C/cm^2). The CV of the thicker poly-**2** electrodes displayed an n-doping charge/p-doping charge ratio significantly lower than 1. This is related to the slower kinetics of the n-doping process, which is due to slow ionic transport and poor solvation of the n-doped state.[11]

The analysis of the shape of the charge−discharge curves of Figure 6 can provide useful information when they are compared with the CV's of the individual polymers. The cell voltage time curve for a poly-**1**-based capacitor (—) almost corresponds to that expected for an ideal capacitor.[36] On the other hand, the charge−discharge curve for a poly-**3**-based capacitor (- - -) shows a linear decrease between 2 and 1.5 V which is followed by an abrupt decrease. This is reminiscent of a discharge curve for a battery.[36] The abrupt decrease stems from the fact that poly-**3** displays a wide potential range with almost no electroactivity between the n- and p-doped states whereas poly-**1** is almost completely electroactive between −1.3 and 0.6 V versus Ag/Ag$^+$ (Figure 1). Finally, the data of Figure 6 for a poly-**2**-based capacitor (···) differ significantly from the previous ones in that the charge and discharge curves are asymmetrical. This might be due to some irreversible process and degradation of the polymers, since during discharge most of the charge is restored at low cell voltage compared to the case of the charging process.

The power densities exhibited by a poly-**1**- or poly-3-based device are comparable to that reported for a type I symmetric poly(3,4-ethylenedioxythiophene) (PEDOT)-based supercapacitor[37] and a type III poly(dithienothiophene) (PDTT)-based capacitor[6,38,39] at similar discharge times. On the other hand, the power densities of poly-**1**- and -**3**-based capacitors are lower than those of poly(3-(4-fluorophenylthiophene)) (PFPT) and 3-(3,4-difluorophenyl)thiophene (MPFPT).[26] For the last, the discharge current used for the galvanostatic experiment was twice as large and the deposited charge was 60 times larger. The midterm requirements established by the U.S. Department of Energy for supercapacitors (E > 5 W h/kg and P > 500 W/kg, including electrolyte, separator, etc.)[26] can be met by poly-**1**- and -**3**-based supercapacitors, and therefore they make attractive polymer-based supercapacitors even if it remains clear that additional work is required to improve the performance of the capacitors, especially when thicker polymer films are used.

Conclusion

Electrochemical and physical characterization of carbon paper electrodes coated with five polycyanoethylene derivatives was performed. From the cyclic voltammetry data, band gap values between 0.5 and 1.5 eV with an electroactivity window of 2 V were evaluated for poly-**1**−**5**. The polymers were shown by SEM either to have an open and rough morphology (for poly-**1** and -**2**) or to be a thin film with a more compact structure (poly-**3**). The position of the cyano group in the structure of the precursor influences greatly the polymerization efficiency of the resulting polymers. Both poly-**4** and -**5**, having the cyano group close to either the 3-methylthiophene unit or the furan unit, respectively, present low film capacitance and poor cycling stability. This can be attributed to steric hindrance effects for poly-**4** and the irreversibility of the n-doping process for poly-**5**. The last is also chemically unstable in the oxidized state. Capacitors assembled from poly-**1**-, -**2**-, and -**3**-coated carbon paper electrodes showed a significant decrease in discharge capacity during the first 100 cycles. Thus, it is clear that the stability of such low band gap polythiophene-based capacitors has to be improved. It has already been shown that electrolyte impurities, oxygen, and water affect the stability of conducting polymers under electrochemical conditions.[40] To minimize these drawbacks, additional work is required to find new solvents and/or new supporting electrolytes.

Experimental Section

Chemicals and Reagents. Acetonitrile from Aldrich was either distilled before use or used as is if the acetonitrile was HPLC grade.

Tetraethylammonium tetrafluoroborate (Et_4NBF_4) (Aldrich, 99%) was recrystallized three times from methanol and dried under vacuum at 140 °C for 12 h prior to use. Furaldehyde, rhodanine, 3-bromothiophene, potassium *tert*-butoxide, 2-thiopheneacetonitrile, 2-thiophenecarboxaldehyde and 3-methyl-2-thiophenecarboxaldehyde were obtained from Aldrich Chemical Co. and were used without further purification.

General Procedure for the Knoevenagel Condensation. To a stirred solution of 2.9 g (23.54 mmol) of thiophenecarboxaldehyde dissolved in 50 mL of ethanol was added 2.64 g (23.54 mmol) of 2-thiopheneacetonitrile, followed by potassium *tert*-butoxide or sodium hydroxide (10% in mole). After 10 min at room temperature, the formation of a yellow precipitate was observed, and after an additional hour of stirring, the solid was filtered, washed twice with ethanol, and dried, to give 4.7 g of **1** as yellow crystals.

General Procedure for the Synthesis of 2-Arylacetonitrile (4 Steps). *Fufuralrhodanine*. To a solution of 3.6 g (37.5 mmol) of furaldehyde and 5 g (37.5 mmol) of rhodanine in 25 mL of hot glacial acetic acid was added 6.5 g of sodium acetate. The reaction mixture was refluxed for 3 h, the crude mixture was poured over 500 mL of water, and the crystals

(36) Conway, B. E. *Electrochemical Supercapacitors*; Kluwer Academic/Plenum: New York, 1999.
(37) Carlberg, J. C.; Inganas, O. *J. Electrochem. Soc.* **1997**, *144*, L61.
(38) Arbizzani, C.; Mastragostino, M.; Meneghello, L. *Electrochim. Acta* **1996**, *41*, 21.
(39) Arbizzani, C.; Mastragostino, M.; Meneghello, L. *Electrochim. Acta* **1995**, *40*, 2223.
(40) Pud, A. A. *Synth. Met.* **1994**, *66*, 1.

were filtered off, washed with water, and then dried under reduced pressure. The yield was 7.72 g (98%) of orange crystals.

3-α-Furyl-2-thioketopropionic Acid. Fufuralrhodanine (6.0 g, 28.4 mmol) was suspended in a stirred solution of 40 mL of sodium hydroxide 15% and heated, with stirring, until all the crystals dissolved (about 1 h). The alkaline solution was cooled to near 0 °C, and the acid rapidly precipitated out upon addition of 40 mL of hydrochloric acid 10%. The precipitate was filtered off, washed well with water, and then dried to yield 4.52 g (94%) of a pale yellow powder.

3-α-Furyl-2-oximinopropionic Acid. A solution of 2.0 g (11.8 mmol) of 3-α-furyl-2-thioketopropionic acid and 1.1 g (39.2 mmol) of hydroxylamine (from 2.5 g of hydroxylamine hydrochloride and 0.9 g of sodium) in 30 mL of absolute ethyl alcohol was refluxed for 45 min, and then the alcohol was removed under reduced pressure. The residual solid mass was dissolved in 25 mL of sodium hydroxide 10% and then filtered. Careful acidification of the cooled filtrate (0−5 °C) with a 30% HCl solution precipitated the product as a light brown powder. The yield was 1.7 g (86%).

2-Furanacetonitrile. A mixture of 2.0 g (11.8 mmol) of oximino acid and 12 mL of acetic anhydride was warmed cautiously until effervescence set in. At the end of the effervescence, the acetic anhydride was removed under reduced pressure and the residue taken up in 20 mL of water and 60 mL of ether. The ethereal layer was washed with sodium carbonate, dried over anhydrous magnesium sulfate, and evaporated under reduced pressure. The product was obtained by distillation to give 0.32 g (25%) of a colorless liquid.

E-α-[(2-thienyl)methylene]-2-thiopheneacetonitrile (**1**). Yield 97%; mp 126 °C; IR (KBr) ν: 3097, 3082, 2211, 1586, 731, 713, 695 cm^{-1}; ^1H NMR ($CDCl_3$) δ: 7.07 (dd, 1H), 7.15 (dd, 1H), 7.30 (dd, 1H), 7.34 (dd, 1H), 7.50 (s, 1H), 7.54 (d, 1H), 7.62 (d, 1H); ^{13}C NMR ($CDCl_3$) δ: 102.93, 116.83, 125.85, 126.74, 127.80, 128.05, 129.83, 131.91, 132.02, 137.39, 138.56; UV ($CHCl_3$) λ_{max}: 368 nm; MS *m*/*z* (%): 217 (M^+, 100%), 190 (11%), 172 (47%), 95 (11%). Anal. Calcd for $C_{11}H_7NS_2$: C, 60.80; H, 3.25; N, 6.45; S, 29.51. Found: C, 60.77; H, 3.23; N, 6.50; S, 29.64.

E-α-[(3-methyl-2-thienyl)methylene]-2-thiopheneacetonitrile (**2**). Yield 85%; mp 88 °C; IR (KBr) ν: 3110, 3093, 2918, 2214, 1584, 733, 712 cm^{-1}; ^1H NMR ($CDCl_3$) δ: 2.40 (s, 3H), 6.94 (d, 1H), 7.07 (dd, 1H), 7.28 (dd, 1H), 7.33 (dd, 1H), 7.44 (d, 1H), 7.55 (s, 1H); ^{13}C NMR ($CDCl_3$) δ: 143.6, 101.67, 117.03, 125.47, 126.38, 128.05, 128.59, 130.23, 130.65, 133.74, 139.23, 142.99; UV ($CHCl_3$) λ_{max}: 374 nm; MS *m*/*z* (%): 231 (M^+, 100%), 215 (15%), 203 (14%), 196 (11%), 186 (39%), 171 (20), 172 (14%). Anal. Calcd for $C_{12}H_9NS_2$: C, 62.30; H, 3.92; N, 6.06; S, 27.72. Found: C, 62.02; H, 3.89; N, 6.06; S, 27.84.

E-α-[(2-furanyl)methylene]-2-thiopheneacetonitrile (**3**). Yield 98%; mp 77 °C; IR (KBr) ν: 3103, 3084, 2214, 1607, 744, 705, 697 cm^{-1}; ^1H NMR ($CDCl_3$) δ: 6.58 (dd, 1H), 7.09 (m, 2H), 7.20 (s, 1H), 7.30 (dd, 1H), 7.37 (dd, 1H), 7.62 (d, 1H); ^{13}C NMR ($CDCl_3$) δ: 102.40, 112.79, 115.10, 116.56, 125.69, 126.02, 126.96, 128.15, 138.62, 144.88, 149.61; UV ($CHCl_3$) λ_{max}: 364 nm; MS *m*/*z* (%): 201 (M^+, 100%), 172 (88%), 146 (15%), 140 (13%). Anal. Calcd for $C_{11}H_7NOS$: C, 65.65; H, 3.51; N, 6.96; S, 15.93. Found: C, 65.54; H, 3.51; N, 6.99; S, 16.02.

E-α-[(2-thienyl)methylene]-2-(3-methylthiophene)acetonitrile (**4**). Yield 52%; oil at ambient temperature; IR (KBr) ν: 3104, 2924, 2209, 1673, 1425, 857, 835, 712 cm^{-1}; ^1H NMR ($CDCl_3$) δ: 2.44 (s, 3H), 6.90 (d, 1H), 7.15 (dd, 1H), 7.21 (d, 1H), 7.41 (s, 1H), 7.54 (d, 1H), 7.62 (d, 1H); ^{13}C NMR ($CDCl_3$) δ: 14.92, 101.41, 117.24, 121.21, 124.5, 127.73, 129.96, 131.74, 132.25, 136.54, 137.02, 137.37; UV ($CHCl_3$) λ_{max}: 358 nm; MS *m*/*z* (%): 231 (M^+, 100%), 216 (39%), 147 (38%), 97 (25%). Anal. Calcd for $C_{12}H_9NS_2$: C, 62.30; H, 3.92; N, 6.06; S, 27.72 Found: C, 62.29; H, 3.94; N, 6.05; S, 27.71.

E-α-[(2-thienyl)methylene]-2-furanacetonitrile (**5**). Yield 70%; mp 60 °C; IR (KBr) ν: 3100, 2214, 1590, 1416, 1048, 744, 721, 707 cm^{-1}; ^1H NMR ($CDCl_3$) δ: 6.50 (dd, 1H), 6.63 (d, 1H), 7.15 (dd, 1H), 7.46 (d, 1H), 7.53 (d, 1H), 7.62 (d, 1H), 7.66 (s, 1H); ^{13}C NMR ($CDCl_3$) δ: 98.97, 103.50, 109.63, 112.37, 127.98, 129.93, 130.34, 131.98, 137.72, 143.56, 148.89; UV ($CHCl_3$) λ_{max}: 369 nm; MS *m*/*z* (%): 201 (M^+, 100%), 172 (66%), 146 (20%). Anal. Calcd for $C_{11}H_7NOS$: C, 65.65; H, 3.51; N, 6.96; S, 15.93. Found: C, 65.50; H, 3.52; N, 6.89; S, 16.01.

Equipment for the Purification and Characterization of the Monomers. Melting points were determined with a Fisher-Johns melting point apparatus and are uncorrected. Infrared spectra were recorded on a Perkin-Elmer 1600 FTIR instrument. ^1H NMR spectra were recorded using a Varian 300 MHz spectrometer. Chemical shifts are reported in parts per million (δ) and the signals have been designated as follows: s (singlet), d (doublet), t (triplet) and m (multiplet). ^{13}C NMR spectra were recorded at 75 MHz. UV-visible spectra were collected with an Hewlett Packard model 8452A spectrophotometer. Mass spectra were obtained using a GC-MS (GCD plus gas chromatography-electron ionization detector, HPG 1800A GCD system) equipped with a 5% crosslinked Ph Me silicone HP 19091 J-433 column. Separations were carried out on silica gel (7749 Merck) using circular chromatography (chromatotron, model 7924, Harrison Research). Elemental analyses were carried out at the Chemistry Department of the Université de Montréal, on a Fisons Instrument SPA, model EA1108.

General Procedure To Determine the Oxidation Potential of Monomers. Experiments were carried out on a PAR 273 Potentiostat-Galvanostat in a three-electrode single-compartment cell. A platinum disk (diameter = 0.05 cm) was used as working electrode and a Pt mesh as counter electrode. All potentials were reported versus a Ag/Ag^+ (10 mM $AgNO_3$, 0.1 M tetrabutylammonium perchlorate, acetonitrile) reference electrode. The solution was made with acetonitrile, 10^{-6} M monomer, and 0.1 M tetraethylammonium tetrafluoroborate (Et_4NBF_4). The oxidation potential peak was determined using the first potential scan (100 mV/s) without polymer formation.

Polymeric Film Electrodeposition. The working electrodes were 0.5 cm × 1 cm and 0.010 in. thick carbon paper (Spectracorp) with a specific surface area of 1−2 m^2/g and indium tin oxide (ITO)-coated glass electrodes. Typically, the weight of the carbon electrode was 6.3 mg. Prior to any measurements, the carbon paper electrodes were washed in methanol in an ultrasonic bath for 1−2 min and dried at 50 °C. The ITO electrodes were washed with acetone. The polymer films were grown from a solution containing 10−90 mM of **1**, **2**, **3**, **4**, or **5** and 1 M Et_4NBF_4 in acetonitrile. The electropolymerization was performed galvanostatically at a current density of 0.1−0.5 mA/cm^2. The films were then washed in acetonitrile in order to remove any soluble species from the film and cycled in a monomer free solution of 1 M Et_4NBF_4 in acetonitrile.

Procedure and Equipment. The morphology and thickness of the deposited films were observed by scanning electron microscopy, SEM, using a Hitachi model S-5300 microscope. Photomicrographs were taken on poly-**1**−**5**-coated carbon paper electrodes. All the films were thoroughly rinsed with CH_3CN prior to analysis.

All measurements were performed in a glovebox under a dry nitrogen atmosphere, in a closed three-electrode cell (except for galvanostatic charge−discharge cycling; see below). Cyclic voltammetric studies were performed using a potentiostat model 1287 Solartron Electrochemical Interface coupled to a PC with Corrware Software for Windows (Scribner Associates, version 1.4). During the electrochemical measurements, a total geometric area of 1 cm^2 (both sides of a 1 cm × 0.5 cm carbon paper electrode) of each electrode was exposed to the electrolytic solution. This total area has been used in reporting our results. For example, low-frequency capacitance values are given in F/cm^2. For values given versus weight (i.e. W h/kg), calculations were made via the expected weight of the conducting polymer electropolymerized on a 1 cm^2 carbon paper electrode (Table 3) by assuming a polymerization efficiency of 100%. Electrochemical impedance measurements were performed with a model 1255 Solartron Frequency Response Analyzer coupled to a model 1287 Solartron Electrochemical Interface. Data were collected and analyzed using a PC and Zplot Software for Windows (Scribner Associates, version 1.4). Electrode potential measurements were made

over a frequency range of 65 kHz to 0.05 Hz using a 10 mV sine-wave amplitude. The polymer electrode was polarized at the appropriate potential for about 50 s before the impedance measurements were taken in order to ensure that the polymer film electrode had reached equilibrium. The UV−visible spectra were recorded on a HP 8452A Diode Array spectrophotometer. Spectra were collected for each monomer in solution ($CHCl_3$) and for the corresponding polymer-coated ITO electrode. For the last, the electrode was polarized at about 0 V versus Ag/Ag^+ using a M 263A potentiostat coupled to a PC with Corrware Software for Windows (Scribner Associates, version 1.4), to undope the polymer before recording spectra. The corresponding potential was determined from the cyclic voltammograms.

The charge−discharge experiments were performed with two polymer-coated carbon paper electrodes separated by about 0.5 cm and placed in a flooded electrolyte cell. A Ag/Ag^+ reference electrode was also used to monitor the potential of each electrode during cycling. For poly-**1** and poly-**3**, following polymer growth, the potential of each electrode was set at about −0.3 V versus Ag/Ag^+ and the capacitor was charged at 0.5 mA/cm^2 from 0 to 2 V. To ensure that the capacitor is fulled charged, the cell voltage was maintained at 2 V for 100 s and the discharge was carried out at 0.5 mA/cm^2. It should be noticed that, following the same procedure, the cycling of poly-**1**-coated carbon paper electrodes was also performed between 0 and −2 V. This cycling procedure was used instead of the more conventional method, which consists of cycling between 0 and an appropriate cell voltage, to determine if an inversion of the polarity of the capacitor would be beneficial. Poly-**2** electrodes were preset at −0.6 V, and the charge−discharge experiment for poly-**2**-coated carbon paper electrodes was only carried out at 0.3 mA/cm^2 without any other additional step in the procedure. When poly-**1** and poly-**2** capacitors were charged, the negative electrode potential reached −1.4 V (+0.6 V for the positive electrode) and −1.6 V (+0.4 V for the positive electrode) for poly-**3**.

Acknowledgment. This research was funded by the National Science and Engineering Research Council through a strategic grant (to L.B. and D.B.). We also wish to acknowledge the financial contribution of UQAM. We thank R. Mineau from UQAM (Département des Sciences de la Terre) for the SEM measurements.

Supporting Information Available: Figures showing cyclic voltammograms of poly-**2** and poly-**4** and geometry optimizations of **1**−**5**. This material is available free of charge via the Internet at http://pubs.acs.org.

CM000011R